

Two-proton correlation function for the $pp \rightarrow pp + \eta$ and $pp \rightarrow pp + pions$ reactions

P. Klaja^{1,2,3,†}, P. Moskal^{2,3,§}, E. Czerwiński^{2,3},
R. Czyżykiewicz³, A. Deloff⁴, D. Gil³, D. Grzonka²,
B. Kamys³, A. Khoukaz⁵, J. Klaja^{2,3}, W. Krzemień^{2,3},
W. Oelert², J. Ritman², T. Sefzick², M. Siemaszko⁶,
M. Silarski³, J. Smyrski³, A. Täschner⁵, M. Wolke²,
J. Zdebik³, M. Zieliński^{2,3}, W. Zipper⁶

¹ Physikalisches Institut, Universität Erlangen–Nürnberg, D-91058 Erlangen, Germany

² Institut für Kernphysik, Forschungszentrum Jülich, D-52425 Jülich, Germany

³ The Marian Smoluchowski Institute of Physics, Jagellonian University, PL-30-059 Cracow, Poland

⁴ The Andrzej Soltan Institute for Nuclear Studies, PL-00-681 Warsaw, Poland

⁵ Institut für Kernphysik, Westfälische Wilhelms–Universität, D-48149 Münster, Germany

⁶ Institute of Physics, University of Silesia, PL-40-007 Katowice, Poland

Abstract. For the very first time, the correlation femtoscopy method is applied to a kinematically complete measurement of meson production in the collisions of hadrons. A two-proton correlation function was derived from the data for the $pp \rightarrow ppX$ reaction, measured near the threshold of η meson production. A technique developed for the purpose of this analysis permitted to establish the correlation function separately for the production of the $pp + \eta$ and of the $pp + pions$ systems. The shape of the two-proton correlation function for the $pp\eta$ differs from that for the $pp(pions)$ and both do not show a peak structure opposite to results determined for inclusive measurements of heavy ion collisions.

PACS numbers: 13.60.Hb, 13.60.Le, 13.75.-n, 25.40.Ve

Submitted to: *J. Phys. G: Nucl. Phys.*

1. Introduction

Momentum correlations of particles at small relative velocities are widely used to study the spatio-temporal characteristics of the production processes in relativistic heavy ion collisions [1]. This technique, called after Lednicky *correlation femtoscopy* [2], originates from photon intensity interferometry initiated by Hanbury Brown and Twiss [3]. Implemented to nuclear physics [2,4,5] it permits to determine the duration of the emission process and the size of the source from which the particles are emitted [2]. A central role plays the correlation function which has been defined as

† e-mail address: p.klaja@fz-juelich.de

§ e-mail address: p.moskal@fz-juelich.de

the measured two-particle distribution normalized to a reference spectrum obtained by mixing particles from different events [2]. The importance of the correlation femtoscopy has been well established for investigations of the dynamics of heavy ion collisions with high multiplicity. However, as pointed out by Chajecski [6], in the case of low-multiplicity collisions the interpretation of correlation function measurements is still not fully satisfactory, especially in view of the surprising observation by the STAR collaboration indicating universality of the resulting femtoscopic radii for both, the hadronic (proton-proton), and heavy ion collisions [7]. One of the challenging issues in this context is the understanding of contributions from non-femtoscopic correlations which may be induced by the decays of resonances, global conservation laws [6], or by other unaccounted interactions. In contrast to heavy ion collisions, in the case of single meson production, the kinematics of all ejectiles may be entirely determined and hence a kinematically complete measurement of meson production in the collisions of hadrons gives access to complementary information which could shed light on the interpretation of the two-proton correlations observed in heavy ion reactions. It is also important to underline that the correlation of protons was never exploited till now in near threshold meson productions, and as an observable different from the distributions of cross sections, it may deepen our understanding of the dynamics of meson production. Particularly favourable are exclusive experiments conducted close to the kinematical threshold where the fraction of the available phase-space associated with low relative momenta between the ejectiles is large [8].

In this article we report on a η meson and multi-pion production experiment in which the mesons were created in collisions of protons at a beam momentum of 2.0259 GeV/c corresponding to an excess energy of $Q = 15.5$ MeV for the $pp \rightarrow pp\eta$ reaction. The measurement of the two-proton correlation function for these reactions is important not only in the context of studying the dynamics underlying the heavy ion physics. Such investigations are interesting by themselves because they offer a new promising diagnostic tool, still not exploited, for studying the dynamics of meson production in hadron collisions.

The correlation function carries information about the emitting source and, in particular, about the size of the interaction volume of the $pp \rightarrow pp\eta$ process. The knowledge of this size might be essential to answer the intriguing question whether the three-body $pp\eta$ system is capable of supporting an unstable Borromean bound state. Borromean systems may be realized in a variety of objects on the macroscopic (e.g. strips of papers), molecular [9,10] and nuclear scale (e.g. ^{11}Li or ^6He nuclei [11–13]). According to Wycech [14], the large enhancement of the excitation function for the $pp \rightarrow pp\eta$ reaction observed close to the kinematical threshold may be explained by assuming that the proton-proton pair is emitted from a large (Borromean like) object whose radius is about 4 fm.

2. Experimental technique

The experiment was conducted using the proton beam of the cooler synchrotron COSY [15] and an internal hydrogen cluster target [16]. Momentum vectors of outgoing protons from the $pp \rightarrow ppX$ reaction were measured by means of the COSY-11 facility [17] presented schematically in Figure 1.

The two-proton correlation function $R(k)$ was determined for the $pp\eta$ and $pp(\text{pions})$ systems, respectively. Here, $R(k)$ denotes a projection of the correlation function onto the momentum of one of the protons in the proton-proton center-of-

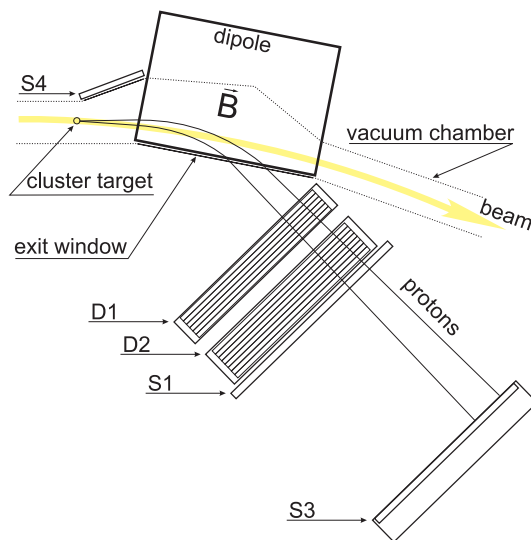


Figure 1. Schematic view of the COSY-11 detection setup [17]. Superimposed lines indicate trajectories of protons from the $pp \rightarrow pp\eta$ reaction. The positively charged particles were identified using the time of flight between the scintillator detectors S1 and S3 combined with a momentum reconstruction by tracking back the trajectories (reconstructed based on the signals from the drift chambers D1 and D2) through the magnetic field of the COSY dipole to the reaction point. The size of the detectors and their relative distances are not to scale. More detailed description can be found in [17–20].

mass system \parallel . It was calculated, by means of the well established technique, as a ratio of the momentum (k) dependent reaction yield $Y(k)$ to the uncorrelated yield $Y^*(k)$ according to the formula (cf. [21])

$$R(k) + 1 = C \frac{Y(k)}{Y^*(k)}, \quad (1)$$

where C denotes an appropriate normalization constant. $Y^*(k)$ was derived from the uncorrelated reference sample obtained by using the event mixing technique introduced by Kopylov and Podgoretsky [5].

The separation of the correlations of the $pp + \eta$ from the $pp + pions$ system and corrections for the limited acceptance of the detection system constitute the two main challenges to be solved when deriving the correlation function from the experimental data.

2.1. Separation of events from the production of $pp\eta$ and $pp + pions$ systems

In the discussed experiment, the four-momenta of the two final state protons were measured only, and the unobserved meson was identified via the missing mass technique [18, 20]. In such situations the entirely accessible information about the reaction is contained in the momentum vectors of the registered protons. Therefore, it is impossible to know whether in a given event the η meson or a few pions have

\parallel Note, that some authors instead of k take as the independent variable the relative momentum of emitted particles $q = |\vec{p}_1 - \vec{p}_2|$ with $k \approx q/2$.

been created. However, statistically one can separate these groups of events using the missing mass spectra for each chosen region of the phase-space.

Thus, $Y_{pp\eta}(k)$ can be extracted for each studied interval of k by grouping the sample of measured events according to the value of k , next calculating the missing mass spectra of the $pp \rightarrow ppX$ reaction for each sub-sample separately, and counting the number of $pp\eta$ events from these spectra. Examples of typical missing mass histograms for three different k intervals are presented in Figure 2. The statistics obtained in the considered measurement allowed to divide the kinematically available range of k into bins whose width ($\Delta k = 2.5 \text{ MeV}/c$) corresponds approximately to the accuracy of the determination of k with ($\sigma(k) \approx 2 \text{ MeV}/c$). A clear signal of η meson production is observed in each spectrum on top of a continuous distribution originating from the multi-pion production. It is important to note that in the studied range of the missing mass the observed shape of the multi-pion distributions is well reproduced in corresponding simulation studies for each region of the phase space [18]. An

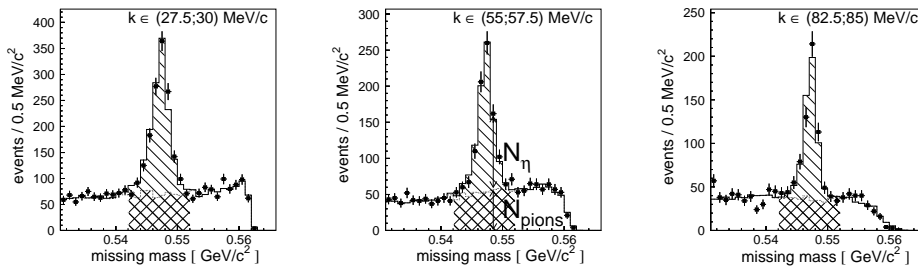


Figure 2. Examples of missing mass spectra measured [20] for the $pp \rightarrow ppX$ reaction at $k \in (27.5; 30.0) \text{ MeV}/c$, $k \in (55.0; 57.5) \text{ MeV}/c$ and $k \in (82.5; 85.0) \text{ MeV}/c$. Points represent experimental data. Dotted histograms depict simulations of the $pp \rightarrow pp2\pi$, $pp \rightarrow pp3\pi$ and $pp \rightarrow pp4\pi$ reactions, while solid line histograms present the sum of simulations for the $pp \rightarrow pp\eta$ reaction and for the $pp \rightarrow pp2\pi$, $pp \rightarrow pp3\pi$ and $pp \rightarrow pp4\pi$ reactions, respectively. The simulated spectra were fitted to the data adjusting only the amplitude [20].

extraction of $Y_{pp\eta}^*(k)$ - unbiased by the multi-pion production - is, however, not trivial. Applying a mixing technique one can construct the uncorrelated reference sample, taking momentum vectors of protons corresponding to different real events. A real event is determined by the momentum vectors of two protons registered in coincidence, and an uncorrelated event will thus comprise momentum vectors of protons ejected from different reactions. Unfortunately, in such a sample of uncorrelated momentum vectors, due to the loss of the kinematical bounds, the production of the η meson will be not reflected on the missing mass spectrum and hence it cannot be used to extract a number of mixed-events corresponding to the production of the η meson. Therefore, in order to determine a background-free correlation function for the $pp \rightarrow pp\eta$ reaction we performed the following analysis: First, for each event, the probability ω was determined that this event corresponds to the $pp \rightarrow pp\eta$ reaction. The probability ω_i , that the i^{th} $pp \rightarrow ppX$ event with a missing mass m_i , and a relative momentum of k_i corresponds to a $pp \rightarrow pp\eta$ reaction was estimated according to the formula:

$$\omega_i = \frac{N_\eta(m_i, k_i)}{N_\eta(m_i, k_i) + N_{pions}(m_i, k_i)}, \quad (2)$$

where N_η stands for the number of the $pp \rightarrow pp\eta$ reactions and N_{pions} is the number

of events corresponding to the multi-pion production with the invariant mass equal to m_i . The values of $N_\eta(m, k)$ and $N_{pions}(m, k)$ were extracted from the missing mass distributions produced separately for each of the studied intervals of k . An example of a missing mass spectrum with pictorial definitions of N_{pions} and N_η is presented in the middle panel of Figure 2. Now having introduced the weights we can calculate also the value of $Y^*(k)$ separately for the $pp\eta$ and $pp(pions)$ final states. We can achieve this by sorting an uncorrelated sample according to the k values similarly as in the case of the correlated events and next for each sub-sample we construct background free $Y_{pp\eta}^*(k)$ distributions as a sum of the probabilities that both protons in an uncorrelated event originate from the reaction where the η meson was created. Specifically, if in a given uncorrelated event denoted by l , one momentum is taken from a real event say $l1$ and the second momentum from another real event $l2$, then the probability that both correspond to reactions where an η was created equals to $\omega_{l1} \cdot \omega_{l2}$, and hence the uncorrelated yield $Y_{pp\eta}^*(k)$ may be constructed from the sum $\sum_l \omega_{l1} \cdot \omega_{l2}$, where l enumerates events in the uncorrelated sub-sample selected for a momentum range k .

Analogously one can calculate $Y_{pp(pions)}^*$ assigning to the event a weight equal to $1 - \omega$.

2.2. Acceptance corrections

As the next necessary step in the data evaluation we corrected the determined yields to account for the finite geometrical acceptance and detection efficiency of the COSY-11 detectors [22]. Hereafter for simplicity by "acceptance" both the geometrical acceptance and detection efficiency will be denoted. The acceptance was calculated as a function of the proton momentum in the proton-proton rest frame k . It was obtained using Monte-Carlo simulations and evaluated according to formula:

$$A(k) = \frac{N_{acc}(k)}{N_{gen}(k)}, \quad (3)$$

where $N_{acc}(k)$ and $N_{gen}(k)$ denote the number of accepted and generated events, respectively. Simulations were performed based on the GEANT-3 packages [23] including the realistic geometry of the detectors and a precise map of the field of the dipole magnet. The momentum and spatial beam spreads, multiple scattering, proton-proton final state interaction [24] and other known physical and instrumental effects were taken into account [17, 18]. Knowing the acceptance [22] it would be straightforward to correct the nominator of equation 1, however the correction of the uncorrelated yield $Y^*(k)$ is not trivial since the momenta of protons in the uncorrelated event originate from two independent real events which in general could correspond to different values of the detector acceptance.

Therefore, in order to derive a correlation function corrected for the acceptance, we have created a sample of data that would have been measured with an ideal detector. For this aim each experimental $pp \rightarrow pp\eta$ event was multiplied by $1/A(k)$. This means that a given reconstructed $pp \rightarrow pp\eta$ event with momentum of k was added to the experimental data sample $1/A(k)$ times.

Based on this corrected data sample we calculated the two-proton correlation function according to equation 1. In order to avoid mixing between the same events, a "mixing step" in the calculations was set to a value bigger than the inverse of the lowest acceptance value. The random repetition of identical combinations was also omitted by increasing correspondingly the "mixing step". In particular, a l^{th} event, from

the acceptance corrected data sample, was "mixed" with a $(1+n)^{th}$ event, where $n > \max(1/A(k))$. If the $(1+1)^{th}$ event was the same as 1^{th} , then this was mixed with a $(1+1+2n)$ event, etc.

2.3. Results and conclusions

The two-proton background-free correlation functions for the $pp \rightarrow pp\eta$ and $pp \rightarrow pp + \text{pions}$ reactions corrected for the acceptances are presented in Figure 3 (full squares). As mentioned in the introduction the shape of the obtained correlation function reflects not only the space-time characteristics of the interaction volume but it may also be strongly modified by the conservation of energy and momentum and by the final state interaction among the ejectiles. In order to estimate the influence on the shape induced by the kinematical bounds we have constructed the correlation functions for both, the $pp \rightarrow pp\eta$ and $pp \rightarrow pp + \text{pions}$ reaction assuming a point-like source using a Monte-Carlo simulation. The results of the simulations are presented in Figure 3 (open squares) and it is apparent that they differ significantly from the experimental correlation function. At the origin the Coulomb repulsion between protons brings the experimental correlation function down to zero.

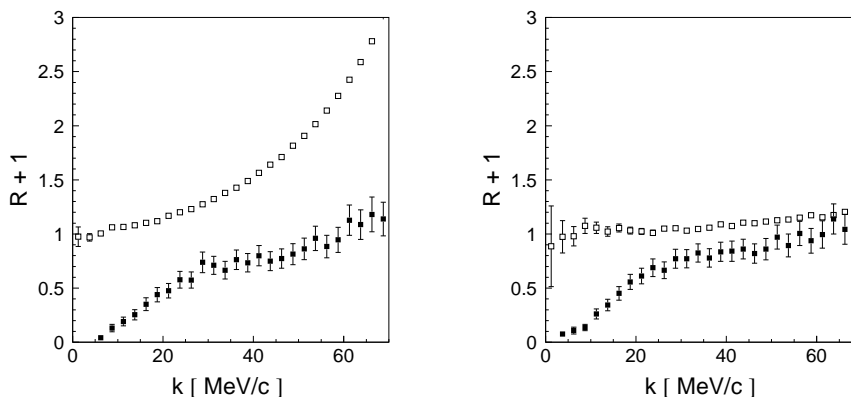


Figure 3. Acceptance corrected experimental proton-proton correlation functions for the production of the η meson (left panel) and multi-pions with the invariant mass equal to the mass of the η meson (right panel). Full squares denote the experimental data and open squares represent results of simulations determined for a point-like source assuming the homogeneous population of the phase space for the reaction products.

Next, in order to extract from the experimental data the shape of the correlation function free from the influence of energy and momentum conservation we constructed a double ratio:

$$R(k) + 1 = Const \left(\frac{Y_{exp}(k)}{Y_{exp}^*(k)} / \frac{Y_{MC}(k)}{Y_{MC}^*(k)} \right), \quad (4)$$

where *Const* denotes the normalization constant, and indices 'exp' and 'MC' refer to the experimental and simulated samples, respectively. The determined double ratios are given in Table 1 and presented in Figure 4. The double ratio is a well established measure of correlations used e.g. by the ALEPH, OPAL and DELPHI collaborations for studying the Bose-Einstein or Fermi-Dirac correlations e.g. in the

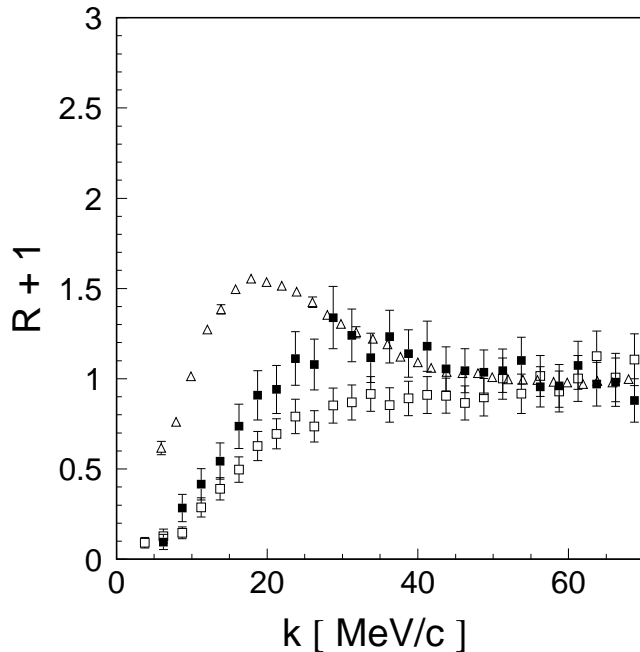


Figure 4. The two-proton acceptance corrected correlation functions normalized to the corresponding simulated correlation function for a point-like source. Results for the $pp \rightarrow pp\eta$ (full squares) and $pp \rightarrow pp + \text{pions}$ (open squares) are compared to the two-proton correlation function determined from heavy ion collisions (triangles) [25].

decays of Z boson [26–28] or W-pairs [29]. In Figure 4 a significant discrepancy between the two-proton correlation functions determined from inclusive heavy ion reactions (triangles) [25] and from exclusive proton-proton measurements (full squares) is clearly visible. The data from the kinematically exclusive measurement do not reveal a peak structure at 20 MeV/c. Although a similar enhancement is also seen in the invariant mass of the proton-proton distributions [20] it disappears in the correlation function for the $pp \rightarrow pp\eta$ and $pp \rightarrow pp + \text{pions}$ reactions.

At present it is not possible to draw a solid quantitative conclusion about the size of the system since e.g. in the case of the $pp \rightarrow pp\eta$ reaction it would require to solve a three-body problem where pp and $p\eta$ [30] interactions are not negligible and both contribute significantly to the proton-proton correlation. However, based on semi-quantitative predictions [31] one can estimate that the system must be unexpectedly large with a radius in the order of 4 fm. This makes the result interesting in context of the predicted quasi-bound ηNN state [32] and in view of the hypothesis [14] that at threshold for the $pp \rightarrow pp\eta$ reaction the proton-proton pair may be emitted from a large Borromean like object whose radius is about 4 fm.

Table 1. The double ratios determined for the production of the η meson and multi-pions with the invariant mass equal to the mass of the η meson. In the first column of the table k denotes the center value of a 2.5 MeV/c interval.

k [MeV/c]	$(R+1)_\eta$	$(R+1)_{pions}$
1.25	—	—
3.75	—	0.09 ± 0.03
6.25	0.10 ± 0.04	0.13 ± 0.04
8.75	0.28 ± 0.08	0.15 ± 0.04
11.25	0.42 ± 0.09	0.29 ± 0.05
13.75	0.54 ± 0.10	0.39 ± 0.06
16.25	0.74 ± 0.12	0.50 ± 0.07
18.75	0.91 ± 0.14	0.63 ± 0.08
21.25	0.94 ± 0.13	0.70 ± 0.08
23.75	1.11 ± 0.15	0.79 ± 0.10
26.25	1.08 ± 0.14	0.74 ± 0.09
28.75	1.34 ± 0.17	0.85 ± 0.10
31.25	1.24 ± 0.15	0.87 ± 0.10
33.75	1.12 ± 0.14	0.92 ± 0.10
36.25	1.23 ± 0.15	0.86 ± 0.09
38.75	1.14 ± 0.13	0.89 ± 0.10
41.25	1.18 ± 0.14	0.91 ± 0.10
43.75	1.06 ± 0.13	0.91 ± 0.10
46.25	1.04 ± 0.12	0.87 ± 0.10
48.75	1.04 ± 0.12	0.90 ± 0.10
51.25	1.04 ± 0.12	1.00 ± 0.11
53.75	1.10 ± 0.13	0.92 ± 0.11
56.25	0.95 ± 0.11	1.02 ± 0.11
58.75	0.96 ± 0.12	0.93 ± 0.11
61.25	1.07 ± 0.13	1.00 ± 0.13
63.75	0.97 ± 0.12	1.13 ± 0.14
66.25	0.98 ± 0.13	1.01 ± 0.13
68.75	0.88 ± 0.12	1.11 ± 0.14

Acknowledgements:

The work was partially supported by the European Community-Research Infrastructure Activity under the FP6 and FP7 programmes (Hadron Physics, RII3-CT-2004-506078, PrimeNet No. 227431), by the Polish Ministry of Science and Higher Education under grants No. 3240/H03/2006/31, 1202/DFG/2007/03, and 0084/B/H03/2008/34, by the German Research Foundation (DFG), and by the FFE grants from the Research Center Jülich, and by the virtual institute "Spin and strong QCD" (VH-VP-231).

- [1] M. A. Lisa *et al* 2005 *Ann. Rev. Nucl. Part. Sci.* **55** 357
- [2] R. Lednicky 2004 *Nukleonika* **49** (Sup. 2) S3
- [3] R. Hanbury Brown and R. Q. Twiss 1954 *Phil. Mag.* **45** 663
- [4] S. E. Koonin 1977 *Phys. Lett. B* **70** 43
- [5] G. I. Kopylov, M. I. Podgoretsky 1972 *Sov. J. Nucl. Phys.* **15** 219
- [6] Z. Chajeccki 2007 *Eur. Phys. J. C* **49** 81
- [7] Z. Chajeccki, M. Lisa 2007 *Braz. J. Phys.* **37** 1057
- [8] P. Moskal, M. Wolke, A. Khoukaz, W. Oelert 2002 *Prog. Part. Nucl. Phys.* **49** 1
- [9] K. S. Chichak *et al.* 2004 *Science* **304** 1308
- [10] S. J. Cantrill *et al.* 2005 *Acc. Chem. Res.* **38** 1
- [11] M. V. Zhukov *et al.* 1993 *Phys. Rept.* **231** 151
- [12] F. M. Marqués *et al.* 2001 *Phys. Rev. C* **64** 061301(R)

- [13] C. A. Bertulani, M. S. Hussein 2007 *Phys. Rev. C* **76** 051602
- [14] S. Wycech 1996 *Acta Phys. Polon.* **B 27** 2981
- [15] D. Prasuhn *et al* 2000 *Nucl. Instr. and Meth.* **A 441** 167
- [16] H. Dombrowski *et al* 1997 *Nucl. Instr. and Meth.* **A 386** 228
- [17] S. Brauksiepe *et al* 1996 *Nucl. Instr. and Meth.* **A 376** 397; P. Klaja *et al* 2005 *AIP Conf. Proc.* **796** 160; J. Smyrski *et al* 2005 *Nucl. Instr. and Meth.* **A 541** 574; P. Moskal *et al* 2001 *Nucl. Instr. and Meth.* **A 466** 448
- [18] P. Moskal 2004 *e-Print Archive: hep-ph/0408162*
- [19] J. Smyrski *et al* 2000 *Phys. Lett.* **B 474** 182
- [20] P. Moskal *et al* 2004 *Phys. Rev. C* **69** 025203
- [21] D. H. Boal *et al* 1990 *Rev. Mod. Phys.* **62** 553
- [22] P. Klaja, P. Moskal and A. Deloff 2007 *AIP Conf. Proc.* **950** 156
- [23] 1994 CERN Application Software Group, GEANT 3.2, CERN Program Library Writeup Report No. W5013
- [24] P. Moskal *et al* 2000 *Phys. Lett.* **B 482** 356; P. Moskal *et al* 2000 *Phys. Lett.* **B 474** 416
- [25] G. Verde, A. Chbihi, R. Ghetti, J. Helgesson 2006 *Eur. Phys. J.* **A 30** 81
- [26] R. Barate *et al* 2000 *Phys. Lett.* **B 475** 395
- [27] P. Abreu *et al* 2000 *Phys. Lett.* **B 471** 460
- [28] G. Abbiendi *et al* 2007 *Eur. Phys. J.* **C 52** 787
- [29] R. Barate *et al* 2000 *Phys. Lett.* **B 478** 50
- [30] S. Wycech and A.M. Green 2005 *Phys. Rev. C* **71** 014001; *ibid* 2005 **C 72** 029902
- [31] A. Deloff 2007 *AIP Conf. Proc.* **950** 150
- [32] T. Ueda 1992 *Phys. Lett.* **B 291** 228